JOURNAL OF VIROLOGY, Dec. 2010, p. 12274–12284 Vol. 84, No. 23
0022-538X/10/$12.00 doi:10.1128/JVI.00260-10

Respiratory Syncytial Virus Induces Host RNA Stress Granules To Facilitate Viral Replication▽

Michael E. Lindquist,[1] Aaron W. Lifland,[4] Thomas J. Utley,[2] Philip J. Santangelo,[4] and James E. Crowe, Jr.[1,2,3]*

Departments of Microbiology and Immunology[1] and Pediatrics[2] and the Vanderbilt Vaccine Center,[3] Vanderbilt University Medical Center, Nashville, Tennessee 37232, and Department of Biomedical Engineering, Georgia Institute of Technology and Emory University, Atlanta, Georgia 30332[4]

Received 4 February 2010/Accepted 8 September 2010

Mammalian cell cytoplasmic RNA stress granules are induced during various conditions of stress and are strongly associated with regulation of host mRNA translation. Several viruses induce stress granules during the course of infection, but the exact function of these structures during virus replication is not well understood. In this study, we showed that respiratory syncytial virus (RSV) induced host stress granules in epithelial cells during the course of infection. We also showed that stress granules are distinct from cytoplasmic viral inclusion bodies and that the RNA binding protein HuR, normally found in stress granules, also localized to viral inclusion bodies during infection. Interestingly, we demonstrated that infected cells containing stress granules also contained more RSV protein than infected cells that did not form inclusion bodies. To address the role of stress granule formation in RSV infection, we generated a stable epithelial cell line with reduced expression of the Ras-GAP SH3 domain-binding protein (G3BP) that displayed an inhibited stress granule response. Surprisingly, RSV replication was impaired in these cells compared to its replication in cells with intact G3BP expression. In contrast, knockdown of HuR by RNA interference did not affect stress granule formation or RSV replication. Finally, using RNA probes specific for RSV genomic RNA, we found that viral RNA predominantly localized to viral inclusion bodies but a small percentage also interacted with stress granules during infection. These results suggest that RSV induces a host stress granule response and preferentially replicates in host cells that have committed to a stress response.

Respiratory syncytial virus (RSV) is a leading cause of serious viral lower respiratory tract illness in infants and the elderly worldwide. The virus is a member of the *Paramyxoviridae* family, and the genome consists of a single-stranded, negative-sense RNA molecule that encodes 11 proteins. The ribonucleoprotein complex necessary for transcription and replication includes the nucleoprotein (N), the phosphoprotein (P), and the large polymerase protein (L). M2-1 and M2-2 are accessory proteins that are involved in transcription and replication, respectively (7). The fusion (F) protein, attachment protein (G), and small hydrophobic (SH) protein are found on the surface of infectious virions, while the matrix (M) protein locates inside the virion particle. Two nonstructural proteins (NS1 and NS2) are expressed in the cytoplasm of infected cells and appear to act as interferon antagonists during infection (36). The mechanisms by which the virus replicates and assembles in infected epithelial cells are incompletely understood.

A hallmark feature of RSV infection in epithelial cells is the formation of discrete collections of viral replication proteins that have been termed viral inclusion bodies (28). These cytoplasmic structures increase in size during the course of infection and have been shown to contain the N, P, M2-1, L, and M proteins (3, 9, 21). It is thought that N and P are the minimal requirements for inclusion body formation, since the expression of both of these proteins in the absence of virus infection induces the formation of inclusion bodies similar to those observed during infection (10). The host proteins Hsp70 and actin associate with RSV inclusion bodies (1), but a functional role for either of these proteins in inclusion bodies is unknown. Although a function has not been defined experimentally for inclusion bodies, it has been proposed that these structures may represent sites of replication and/or transcription for the virus (32).

Stress granules are host RNA cytoplasmic granules formed in cells in response to multiple types of environmental stress (14). The best-studied pathway for stress granule formation involves phosphorylation of the translation initiation factor eIF2α, leading to the accumulation of stalled translation preinitiation complexes (19). RNA transcripts are bound by mRNA binding proteins, including TIA-1, Ras-GAP SH3 domain-binding protein (G3BP), and HuR. Several translation factors, such as eIF4E and eIF3, are recruited to stress granules, resulting in protein-RNA complexes that form the contents of the granules (14). Stress granules can also be induced by an alternate mechanism that is independent of eIF2α phosphorylation via inactivation of the translation factors eIF4A or eIF4G (5, 25).

Many viruses are known to modulate host translation in order to facilitate viral protein production. In recent years, several viruses have been studied to monitor their effect on the host stress response. Viruses that are known to induce host stress granules include the paramyxovirus Sendai virus, the coronavirus mouse hepatitis virus, the alphavirus Semliki Forest virus, reovirus, and poliovirus (12, 24, 30, 34, 39). Although

* Corresponding author. Mailing address: The Vanderbilt Vaccine Center, Vanderbilt University Medical Center, T-2220 MCN, Nashville, TN 37232-2905. Phone: (615) 343-8064. Fax: (615) 343-4456. E-mail: james.crowe@vanderbilt.edu.

▽ Published ahead of print on 15 September 2010.

both poliovirus and Semliki Forest virus induce stress granules early after infection, both viruses appear to functionally inhibit stress granule formation at later time points. In addition, West Nile virus prevents stress granule formation throughout infection (6). While it is reasonable to think that stress granules may play a role in infection for these viruses, the specific role or function of stress granules during infection has not been well defined.

Stress granule proteins also have been shown to interact directly with viral processes. Sindbis virus and vaccinia virus recruit the stress granule protein G3BP to viral structures (4, 13), while West Nile virus interacts with the host stress granule proteins TIA-1 and TIAR (6). Sendai virus trailer RNAs have been shown to bind TIAR (12), and the poliovirus 3C proteinase has been shown to cleave G3BP (39). HuR has been shown to associate with regions of hepatitis C virus (HCV) RNA and the reverse transcriptase protein of human immunodeficiency virus (31, 35).

In the present study, we sought to determine whether the pneumovirus RSV initiates a stress response. Our results demonstrate that RSV induces a robust stress response that continues throughout the course of infection, indicating that RSV may specifically initiate and maintain the stress response. Interestingly, we show that cells that have formed stress granules contain more RSV protein than cells without stress granules. Our data show that, while RSV inclusion bodies are distinct from stress granules, the stress granule marker HuR appears to be a shared component between both structures. In addition, we created a stable cell line deficient for the stress granule assembly protein G3BP. RSV replication in these cells was diminished, offering further evidence that stress granule formation enhances RSV replication. Finally, we show that RSV genomic RNA is strongly associated with RSV inclusion bodies while only a transient interaction occurs with stress granules. This evidence suggests that RSV inclusion bodies and not host stress granules are the active sites of viral replication.

MATERIALS AND METHODS

Cells. HEp-2 cells (ATCC CCL-23) were maintained in Opti-MEM I medium (Invitrogen) containing 5% (vol/vol) fetal calf serum, 1% (vol/vol) L-glutamine, 2.5 μg/ml amphotericin B, and 50 μg/ml gentamicin. MA104 cells (ATCC CRL 2738.1), which were used to prepare rotavirus, and RGD3 and U2OS cells (kindly provided by Paul Anderson, Brigham and Women's Hospital) were maintained in Dulbecco's modified Eagle's medium (DMEM) containing 5% (vol/vol) fetal calf serum, 1% (vol/vol) sodium pyruvate, 1% (vol/vol) L-glutamine, 1% (vol/vol) nonessential amino acids, 2.5 μg/ml amphotericin B, and 50 μg/ml gentamicin.

Viruses. A suspension of RSV wild-type strain A2 prepared in HEp-2 cells (1×10^6 PFU/ml) was used to infect HEp-2 cell monolayer cultures. Infectious virus was adsorbed to the cells for 1 h in a 37°C incubator in 5% CO_2. Following adsorption, the inoculum was removed and fresh medium added. The cells were then incubated at 37°C in 5% CO_2 for the duration of the infection period. UV-inactivated virus was prepared from the same virus stock by irradiation in a UV cross-linker for 15 min. Rhesus rotavirus was a kind gift from Susana Lopez.

Fixation and immunostaining. Cells were fixed with 3.7% (wt/vol) paraformaldehyde in phosphate-buffered saline (PBS) for 10 min at room temperature. Cells were permeabilized with 0.2% (wt/vol) Triton X-100 and 3.7% paraformaldehyde in PBS for 10 min at room temperature. Following fixation, cells were blocked in 5% (wt/vol) bovine serum albumin (BSA) in PBS for 1 h, followed by the addition of the primary antibody for 1 h. Cells were then washed three times in PBS, and species-specific IgG Alexa Fluor (Molecular Probes) was added at a dilution of 1:1,000 in blocking solution to detect primary antibodies. Cells were washed 3 times in PBS and fixed on glass slides using a Prolong antifade kit (Molecular Probes). Images were obtained on a Zeiss inverted LSM510 confocal microscope using a 40× Plan-Neofluar oil objective lens. Polyclonal anti-G3BP (ab37906) antibody was obtained from Abcam and used for immunostaining. The following antibodies were obtained from Santa Cruz for immunostaining: polyclonal anti-TIA-1 (sc-1751), polyclonal anti-HuR (sc-20694), and polyclonal anti-eIF3η (sc-16377). Anti-RSV P protein (clone 3_5) and anti-RSV N protein (clone B130) monoclonal antibodies were a kind gift of Earling Norrby and Ewa Bjorling. An anti-RSV F protein humanized mouse monoclonal antibody (palivizumab; MedImmune) was obtained from the Vanderbilt Pharmacy. Imaging of the RNA with G3BP and RSV N protein was performed using a 63×/1.4 numerical aperture Plan-Apochromat objective using a Zeiss LSM 510 confocal microscope. For images where three-dimensional z-stacks were obtained, we collapsed the series of fields into an extended view using Volocity imaging software.

RT-PCR. HEp-2 cells were grown on 48-well plates and infected with RSV for the times indicated below. RNA was extracted using an RNeasy mini kit (Qiagen). Reverse transcriptase PCR (RT-PCR) was performed using a OneStep RT-PCR kit (Qiagen) and primer-probe combinations for RSV F, rotavirus VP3, or human glyceraldehyde-3-phosphate dehydrogenase (GAPDH). The normalized cycle threshold (ΔC_T) was calculated for each time point using the following formula: ΔC_T = RSV F C_T − GAPDH C_T. The change in normalized C_T over time ($\Delta\Delta C_T$) was calculated for each condition using the ΔC_T of wild-type cells 2 h postinfection (p.i.) as the initial point of reference for the relative amount of viral RNA: $\Delta\Delta C_T$ = [ΔC_T at x h p.i. ± shRNA] − [ΔC_T in wild-type cells 2 h p.i.], where x equals each specific time point.

shRNA reagents. A stable cell line exhibiting knockdown of HuR expression was generated using a set of three SMARTvector lentiviral small hairpin RNA (shRNA) particles (Dharmacon), along with cells treated with nontargeting shRNA particles. HEp-2 cells were plated into 48-well plates at approximately 50% confluence and transduced with the lentiviral particles according to the manufacturer's protocol. A panel of stable cell lines exhibiting knockdown of G3BP expression was generated using Mission shRNA lentiviral transduction particles (Sigma). HEp-2 cells were plated onto 6-well plates and transduced with lentiviral particles according to the manufacturer's protocol. For selection of each target, cells containing integrated lentivirus sequences were selected using puromycin (5 μg/ml) diluted in medium. Medium containing puromycin was replaced every 3 days until resistant colonies were observed. Puromycin-resistant colonies were isolated using cloning cylinders (Sigma) and tested for target protein expression.

Western blotting. HEp-2 cells were grown on 6-well plates and harvested for protein. Cell lysates were obtained using lysis buffer (50 mM Tris-HCl, 150 mM NaCl, 1% Triton X-100, pH 8.0) containing 0.5% (vol/vol) protease inhibitor cocktail (Sigma) and 1.0% (vol/vol) phosphatase inhibitors (Sigma). The lysates were separated on 4-to-12% NuPAGE bis-Tris gels (Invitrogen) and transferred to nitrocellulose membranes using an iBlot dry blotting system (Invitrogen). The membranes were blocked for 1 h using Odyssey blocking buffer (Li-Cor) diluted 1:1 in PBS. Primary antibodies were diluted in blocking buffer and incubated overnight at 4°C. The membranes were then washed four times in Tris-buffered saline plus 0.2% Tween (TBST) for 5 min each. Li-Cor IRDye 680CW or IRDye 800CW secondary antibodies were diluted 1:5,000 in blocking buffer and added to each membrane for 1 h. The membranes were washed four times in TBST. Bands were imaged and quantitated using an Odyssey infrared imaging system. G3BP protein was detected using a monoclonal antibody from BD Biosciences (611127). GAPDH was detected using a monoclonal antibody from Millipore (MAB374). HuR was detected using a monoclonal antibody from Santa Cruz Biotechnology (sc-5261).

RNA probe and live cell delivery. Single-RNA-sensitive probes (33) designed to target the gene start-intergenic region of the genomic RNA of human RSV were delivered at 30 nM via reversible permeabilization with streptolysin O into separate sets of infected or mock-infected HEp-2 cells at 1, 6, 12, 18, and 24 h p.i. Delivery took approximately 10 min, and 15 min after delivery, the cells were fixed with 3.7% (wt/vol) paraformaldehyde in PBS for 10 min at room temperature. The cells could then be immunostained for G3BP and the RSV N protein as discussed above.

Quantification of imaging. To determine quantitative features of stress granule induction by RSV, HEp-2 cells were plated onto coverslips placed in wells of a 24-well plate. Cells were grown to approximately 75% confluence and were infected with RSV for 0, 6, 12, 16, 20, or 24 h (multiplicity of infection [MOI] of 1). Cells were fixed as described above. Cells were stained with anti-G3BP antibody (BD Transduction Laboratories) diluted 1:1,000 in blocking solution, the anti-RSV F protein antibody palivizumab (MedImmune) diluted 1:10,000 in blocking solution, and the nuclear stain To-Pro-3 iodide (Invitrogen) diluted 1:1,000 in blocking solution for 1 h. Twenty high-powered fields (HPFs) were obtained for each time point. Images were examined using Volocity imaging

software (version 5.1; Improvision). The total number of cells in each HPF was quantified by counting the number of nuclei. We also quantified the number of infected cells by staining for the presence of RSV F protein, the number of cells containing stress granules by staining for the presence of G3BP protein, and the number of infected cells that also contained stress granules per HPF. To calculate the stress granule size in wild-type or G3BP-deficient cells, cells were plated onto coverslips placed in wells of a 24-well plate. The cells were then treated with 0.5 mM arsenite for 15 min. The cells were fixed and stained for G3BP (1:500) and TIA-1 (1:250). Images for 10 HPFs were obtained for each cell line. We then used Volocity imaging software to determine the percentage of cells with stress granules per HPF and the size of each stress granule for those cells containing stress granules. To determine inclusion body number and volume, HEp-2 cells were placed on coverslips in 24-well plates. Cells were infected with RSV for 24 h (MOI = 1.0) and fixed. Cells were stained for inclusion bodies using anti-RSV P protein antibody and for stress granules using anti-G3BP antibody. At least 10 cells containing or not containing stress granules were analyzed for inclusion bodies. Volocity imaging software was used to determine the number and volume of individual inclusion bodies per cell. Volocity was also used to quantify the colocalization of the viral genomic RNA with inclusion bodies (marked by the RSV N protein) or with stress granules, in addition to the colocalization of inclusion bodies with stress granules. Manders overlap coefficients were calculated using voxels generated from three-dimensional reconstructions.

RESULTS

RSV infection induces stress granule formation. We first tested whether RSV infection of epithelial cells induced stress granules. HEp-2 cell monolayer cultures were inoculated with RSV wild-type strain A2 at an MOI of 1 and incubated in liquid medium for 24 h. We then fixed the cells and immunostained them for the stress granule proteins G3BP, eIF3η, or TIA-1. The results in Fig. 1A (first column) show that each of these markers frequently relocalized into dense cytoplasmic foci that are characteristic of stress granules. We noted that the host stress granules appeared similar in size, shape, and location to previously described viral inclusion bodies that form during RSV infection. To investigate whether the granules containing stress granule-associated proteins were viral inclusion bodies, we costained infected cells with antibodies to stress granule markers and one of the viral proteins found in inclusion bodies (RSV P protein) (Fig. 1A, middle column). The results indicate that viral inclusion bodies are spatially separated from stress granules and represent distinct structures in the cytoplasm.

We next performed a time course of infection to determine the kinetics of stress granule formation in RSV-infected cells. We inoculated cells with RSV (MOI = 1) and then incubated them for various times (0 to 24 h). We fixed and immunostained cells for RSV F protein and the stress granule protein marker G3BP. After 12 h, stress granules formed, and the number of infected cells containing stress granules increased incrementally throughout the 24-h period of observation (Fig. 1B). We did not observe stress granules in mock-infected cells over the time course. In addition, in the cultures in which RSV was added, we did not observe stress granules in cells that did not stain for RSV protein (data not shown). These results demonstrated that RSV induces a potent stress granule response beginning at about 12 h after inoculation and continuing throughout the viral life cycle. In order to verify that RSV replication is necessary for stress granule formation, we mock inoculated cells, inoculated cells with replication-competent RSV (MOI = 1.0), or inoculated cells with an equivalent volume of UV-inactivated RSV for 48 h and then fixed and immunostained them for RSV F and G3BP. RSV infection once again induced robust stress granule formation (Fig. 2, bottom row), while we did not observe stress granules in mock-inoculated or UV-inactivated RSV-inoculated samples (Fig. 2, top and middle rows). These results confirmed that RSV replication and not simply the presence of RSV protein is required for stress granule formation.

We next compared RSV protein levels between cells with and without stress granules. HEp-2 cells were inoculated with RSV (MOI = 1.0) for 24 h and then fixed and immunostained for RSV P and G3BP. We used RSV inclusion body size and number as a measure to compare the amounts of viral protein present in cells. Interestingly, the results indicated that infected cells that have formed stress granules contain more inclusion bodies than cells that have not formed stress granules (Fig. 3A). In addition, individual inclusion bodies were larger in cells that had formed stress granules (Fig. 3B) and the total amount of protein contained in inclusion bodies was greater (Fig. 3C). Although quantification of the size and number of inclusion bodies in infected cells in the cultures clearly showed larger and more inclusion bodies in cells with stress granules, we also did observe some individual cells without stress granules that contained large amounts of RSV protein (for example, two cells with high N expression in Fig. 7, at 12 h postinfection). These data suggested that stress granules enhance viral protein production and inclusion body formation but are not absolutely required for these viral processes.

Inhibition of host stress granule formation reduces RSV replication. To investigate whether stress granule formation is beneficial to the virus or the host, we inoculated mouse embryo fibroblast (MEF) lines derived from TIA-1- or TIAR-deficient mice (kindly provided by Paul Anderson); however, RSV did not establish a productive infection in these cells (data not shown). It is well established that human RSV strains do not infect murine cells efficiently. Next, we created human cell lines deficient for stress granule formation by transducing HEp-2 cells with lentiviral shRNA transduction particles to induce stable knockdown of G3BP expression. When analyzed by Western blotting, G3BP was not detected in the knockdown cells (Fig. 4A). However, when these cells were compared with wild-type cells by immunofluorescence, we could still observe a small amount of G3BP in fixed and permeabilized knockdown cells. The G3BP-deficient cells expressed normal amounts of other stress granule proteins, such as TIA-1 (Fig. 4B). G3BP-deficient cells were treated with 0.5 mM arsenite for 15 min to determine if they were capable of forming stress granules. Stress granules were detected using anti-TIA-1 antibodies (Fig. 4C). We compared the percentages of cells with stress granules per high-powered field. In G3BP-deficient cells, approximately 75% fewer cells per HPF formed stress granules. We also examined individual G3BP knockdown cells that did form stress granules and noted that there was also a slight decrease in stress granule size compared to those in wild-type HEp-2 cells. These results indicated that G3BP-deficient cells are impaired for stress granule formation.

We next determined whether RSV replication was altered in the G3BP-deficient cell line. Wild-type or G3BP-deficient cells were infected with RSV (MOI = 1) for 1, 2, or 4 days. Cell-associated and supernatant virus were collected separately, and viral titers were determined using plaque assays. The G3BP-deficient cells consistently demonstrated a 10-fold reduction in

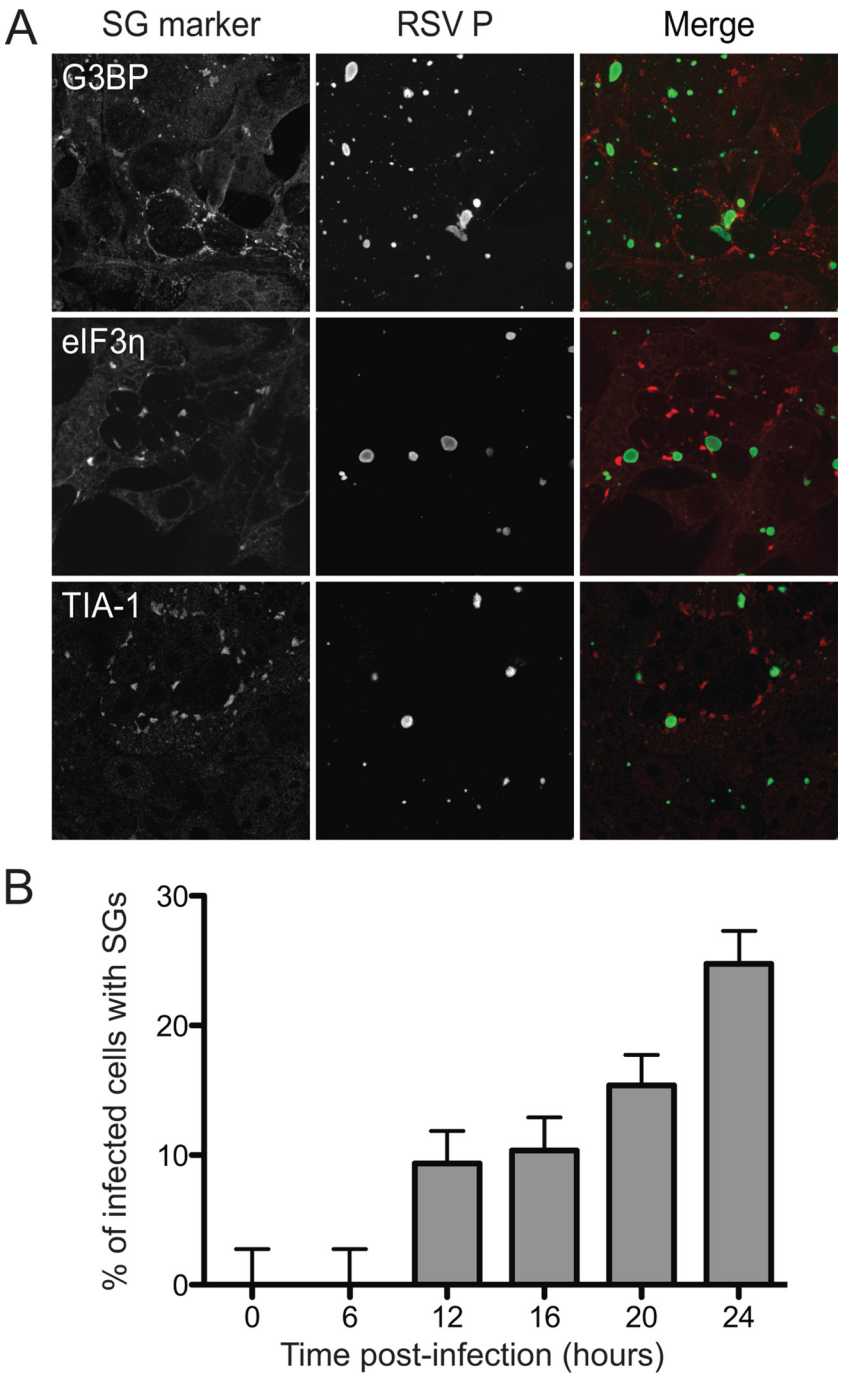

FIG. 1. Stress granules (SGs) are induced during RSV infection. (A) HEp-2 cells were infected with RSV (MOI = 1.0) for 24 h, fixed, and processed for immunofluorescence. Anti-G3BP, anti-eIF3η, and anti-TIA-1 were used as stress granule markers and appear red in the merged image. Anti-RSV P was used as the viral inclusion body marker and appears green in the merged image. The collapsed z-sections are shown for each image. (B) HEp-2 cells were infected with RSV (MOI = 1.0) for the indicated times. The percentages of infected cells and cells containing stress granules per HPF were quantified as described in Materials and Methods. Error bars show standard deviations.

viral titer when comparing supernatant or cell-associated virus with the titers collected from wild-type cells (Fig. 5A). In addition, RSV infection was associated with the death of most wild-type HEp-2 cells after 2 days, while in contrast, the G3BP-deficient cells consistently remained viable for 4 days after infection. We next sought to determine if the reduction of G3BP expression and stress granule formation affected the efficiency of replication of viral RNA. We infected wild-type or G3BP-deficient cells for 0, 2, 12, 24, or 48 h and then harvested total RNA from cell lysates. We performed reverse transcriptase PCR and normalized the RNA levels to that of host GAPDH and compared them with the levels found at 2 h

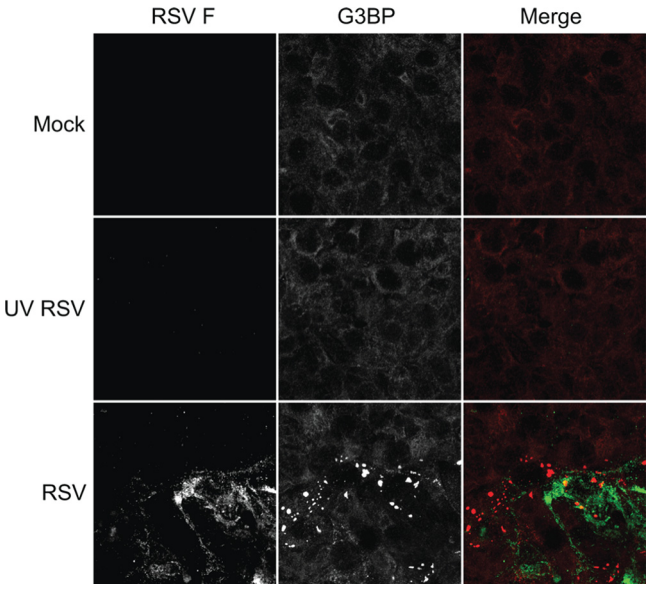

FIG. 2. RSV-induced stress granule formation is dependent on virus replication. HEp-2 cells mock infected (top row), inoculated with replication-competent RSV (MOI = 1.0), or inoculated with UV-inactivated RSV for 48 h were fixed and processed for immunofluorescence. Anti-G3BP was used as a marker for stress granules and appears red in the merged image. Anti-RSV F was used as a marker for viral infection and appears green in the merged image. The collapsed z-sections are shown for each image.

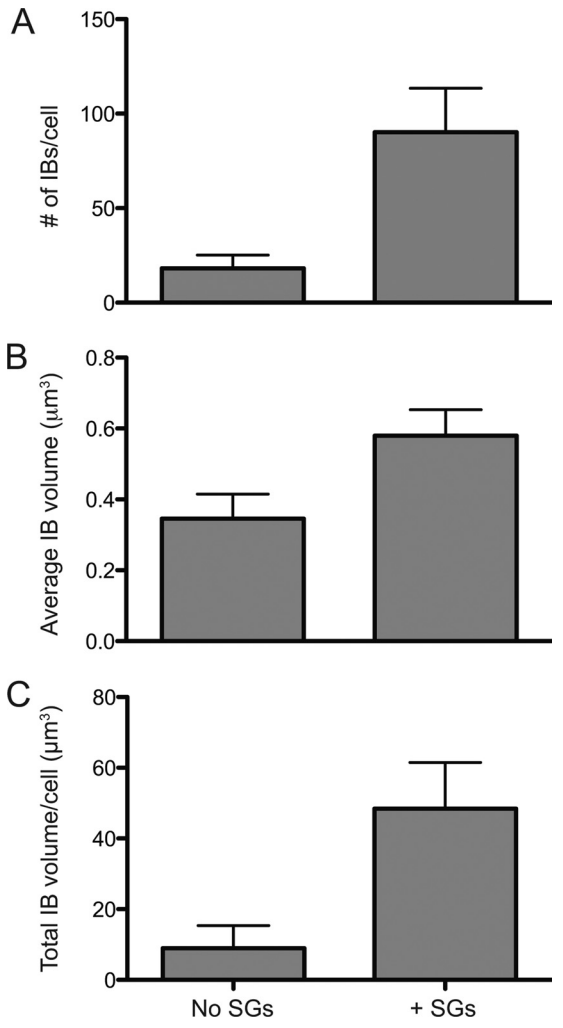

FIG. 3. RSV protein levels are higher in cells with stress granules. HEp-2 cells were infected with RSV (MOI = 1.0) for 24 h. At least 10 infected cells containing or not containing stress granules were analyzed. (A) The total average number of inclusion bodies (IBs) per cell was determined as described in Materials and Methods for cells containing stress granules (+SGs) or not containing stress granules (No SGs). (B) The average volumes (μm^3) of individual inclusion bodies were determined for cells containing or not containing stress granules. (C) The volumes of all individual inclusion bodies in single cells containing or not containing stress granules were totaled on a per cell basis to determine average total inclusion body volume per cell. Error bars show standard deviations.

postinfection in the wild-type HEp-2 cells. We observed a decrease in RSV RNA in the G3BP-deficient cell line at each time point tested after infection (Fig. 5B). Interestingly, when these cells were infected with rhesus rotavirus, a virus that does not induce stress granule formation (27), the replication of rotavirus was unaffected. These data indicate that stress granule formation may play an important role in the RSV life cycle even at very early time points after infection.

We also determined the effects of G3BP overexpression on RSV replication using RGD3 cells, a U2OS osteosarcoma cell line selected to express green fluorescent protein-G3BP. We inoculated RGD3 or parental U2OS cells with RSV (MOI = 1.0) and harvested cell-associated virus for plaque assays at time points spanning 0 to 4 days after inoculation. RSV replication remained largely unaltered in cells overexpressing G3BP (Fig. 5C). Interestingly, although G3BP levels are higher in RGD3 cells, stress granule formation is largely unaltered (18). These data indicated that the presence of artificially elevated levels of G3BP do not enhance replication.

The stress granule marker HuR is recruited to RSV inclusion bodies. We examined other markers of stress granules and found a nonclassical feature involving the mRNA binding stress granule protein HuR. In cells infected with RSV, HuR was recruited to stress granules during infection but the protein was also largely associated with structures that were not marked by other stress granule proteins. When cells were infected (MOI = 1) and costained for G3BP and viral proteins in RSV inclusion bodies, we noted that HuR was present both in host stress granules and in RSV inclusion bodies (Fig. 6A). Thus, HuR protein is a shared component of the two structures. Using RNA interference, we sought to determine the effect of decreased HuR expression on RSV replication. shRNA knockdown of HuR resulted in an approximately 70% reduction of HuR expression when compared by Western blotting to its expression in wild-type cells or cells transduced with a nontargeting shRNA (Fig. 6B). In contrast to G3BP knockdown, stress granule formation was not altered by HuR reduction when cells were treated with sodium arsenite (data not shown). To test whether HuR plays a role in RSV infection, we infected wild-type HEp-2- or HuR-deficient cells with RSV (MOI = 0.1) for 1, 2, 3, or 4 days. Supernatant and cell-associated virus were collected separately at each time point, and viral titers were determined by plaque assay. As shown by the results in Fig. 6D, we did not observe a significant change

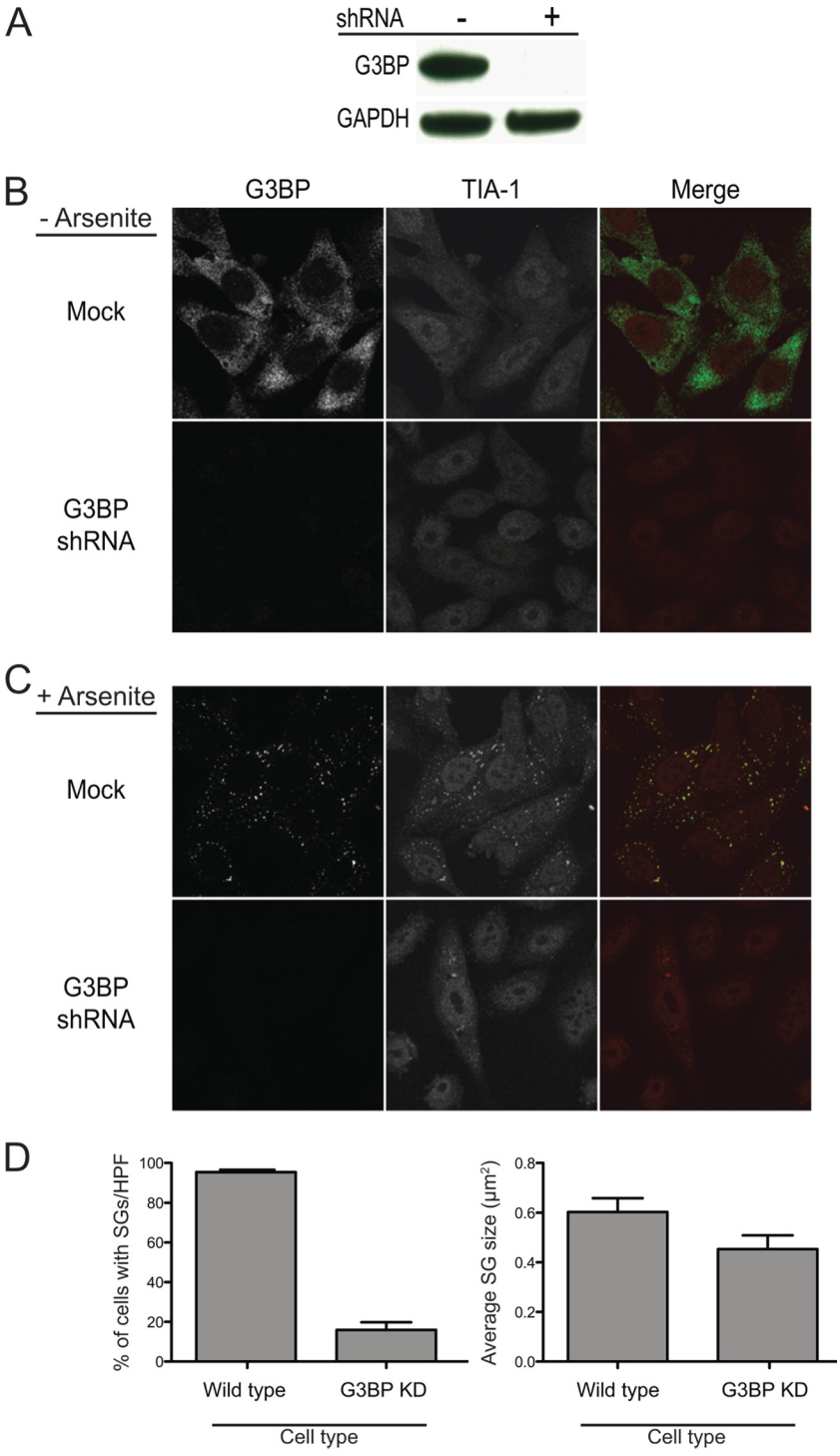

FIG. 4. Decreased levels of G3BP inhibit stress granule formation. (A) Wild-type or representative G3BP-deficient HEp-2 cells were analyzed for G3BP expression via Western blotting. (B) Wild-type or G3BP-deficient HEp-2 cells not treated with arsenite were analyzed for G3BP (green in merged image) and TIA-1 (red in merged image) expression using indirect immunofluorescence. (C) Wild-type or G3BP-deficient HEp-2 cells were treated with arsenite, fixed, and processed for immunofluorescence. Stress granule proteins were stained using anti-G3BP (green in merged image) and TIA-1 (red in merged image) antibodies. (D) Each cell type was examined for the percentage of cells containing stress granules per HPF and the size of stress granules per cell using TIA-1 as a marker for stress granules, as described in Materials and Methods. Error bars show standard deviations. KD, knockdown.

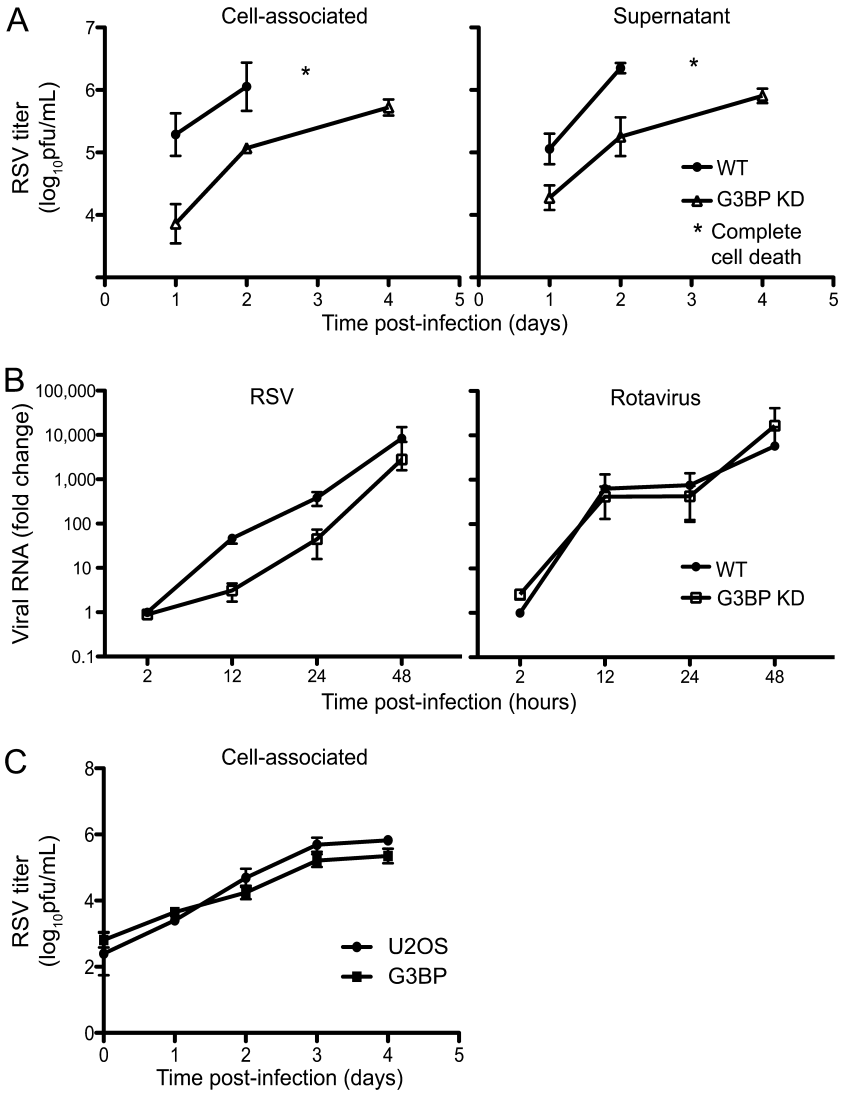

FIG. 5. RSV replication is inhibited in G3BP-deficient cells. (A) Wild-type (WT) or representative G3BP-deficient cells were infected with RSV (MOI = 1.0) for indicated times. Cell-associated or supernatant virus was collected at each time point. Viral titer for each sample was determined by plaque assay. (B) Wild-type or G3BP-deficient cells were infected with RSV or rotavirus for indicated times. Viral RNA was collected and assayed for fold change of RNA during infection. (C) Wild-type or G3BP-overexpressing cells derived from U2OS cells (RGD3) were infected with RSV (MOI = 1.0) for indicated times. Cell-associated virus was collected at each time point, and viral titer for each sample was determined by plaque assay. Error bars show standard deviations.

in viral titer for supernatant or cell-associated virus during infection in HuR-deficient cells. In addition, we monitored for any changes in RSV RNA levels. Wild-type or HuR-deficient cells were infected (MOI = 0.1) for the times stated above, and RNA was harvested. We again performed quantitative RNA studies. As shown by the results in Fig. 6C, we did not find significant differences in RSV RNA levels when HuR expression was reduced. These data, combined with our viral titer results, indicate that the wild-type level of HuR expression is not essential for viral replication even though a significant amount of HuR is recruited to inclusion bodies.

RSV genomic RNA is partially localized to stress granules. Previous reports using fluorescent molecular beacons specific for RSV genomic RNA suggested that RSV RNA could be found in RSV inclusion bodies during infection (32). In addition, more recent studies have shown that RSV RNA transiently interacts with arsenite-induced stress granules as well (33). Using a probe specific for RSV genomic RNA, we sought to determine whether RSV RNA could be found in RSV-induced stress granules, as well as RSV inclusion bodies. HEp-2 cells were infected with RSV (MOI = 1) for 1, 6, 12, and 24 h. After infection, cells were reversibly permeabilized with streptolysin O and incubated with fluorescently labeled RNA probes. Cells were then fixed with paraformaldehyde and stained with a monoclonal RSV N antibody to identify inclusion bodies and a monoclonal anti-G3BP antibody to identify stress granules (Fig. 7). Using confocal microscopy, we then examined the localization of viral RNA at each time point. We observed colocalization between RSV inclusion bodies and viral RNA at all time points, 1, 12, and 24 h after infection, as

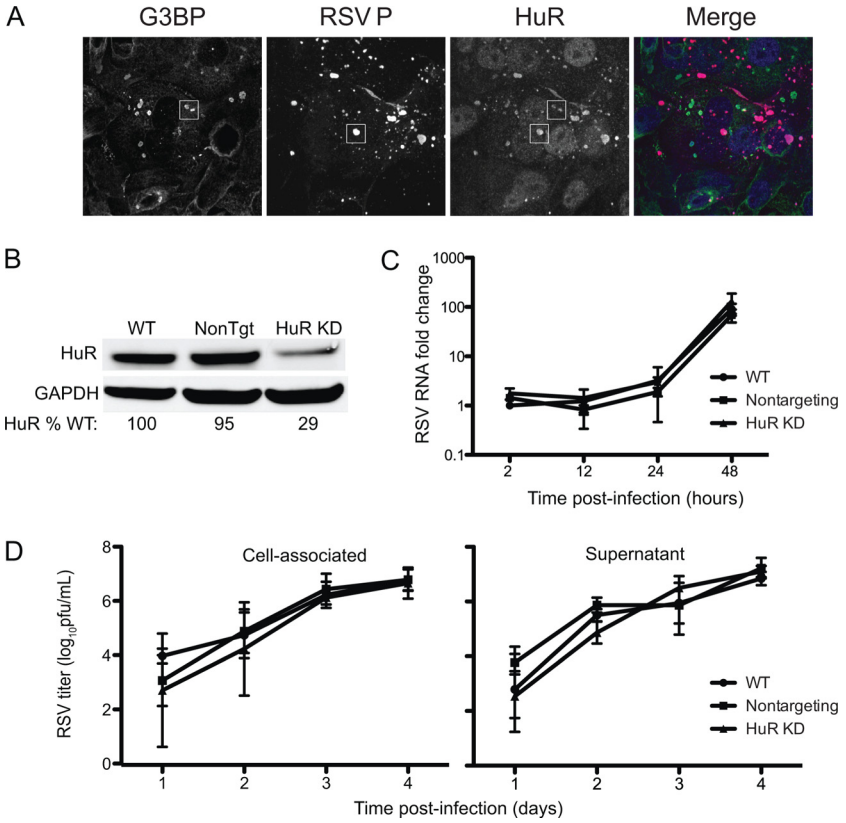

FIG. 6. HuR protein colocalizes with RSV inclusion bodies but is not necessary for replication. (A) HEp-2 cells were infected with RSV (MOI = 1.0) for 24 h, fixed, and prepared for immunofluorescence. Anti-G3BP was used to mark stress granules and appears green in the merged image. Anti-RSV P was used to mark RSV inclusion bodies and appears red in the merged image. HuR appears blue in the merged image. White squares are used to mark areas in which HuR is contained in stress granules or inclusion bodies, respectively. The collapsed z-sections are shown for each image. (B) Cells transduced with nontargeting (NonTgt) or HuR shRNA were compared with wild-type HEp-2 cells for expression levels of HuR. Total HuR levels were quantified for each cell type and compared to wild-type levels. (C) Wild-type HEp-2 cells, cells treated with nontargeting shRNA, or HuR-deficient cells were infected with RSV (MOI = 0.1) for the indicated times. Viral RNA was collected and assayed for the fold change in RNA levels during infection. (D) Wild-type or HuR-deficient cells were infected with RSV (MOI = 0.1) for the indicated times. Cell-associated virus and supernatant virus were collected at each time point. The viral titer for each sample was determined by plaque assay. Error bars show standard deviations.

shown in Fig. 7. Using Volocity imaging software, we determined the average Manders overlap coefficients for inclusion bodies with viral RNA, inclusion bodies with stress granules, and viral RNA with stress granules, utilizing three fields of approximately 35 cells (Table 1). For viral RNA and inclusion bodies, the Manders overlap coefficients were 0.87, 0.96, and 0.91 (87, 96, and 91% overlap) for 1, 12, and 24 h after infection, respectively. For the inclusion bodies with stress granules, the average Manders overlap coefficients were 0.0, 0.016, and 0.034 (0 [no stress granules], 1.6, and 3.4% overlap), likely representing a transient interaction. For the viral RNA with stress granules, the average Manders overlap coefficients were 0.0, 0.022, and 0.045 (0 [no stress granules], 2.2, and 4.5% overlap), also likely representing a transient interaction. In addition, we show the overlapping intensity profiles of the viral RNA, inclusion bodies, and stress granules (as visualized in intensity profiles in the fifth column of Fig. 7) to demonstrate the amount of colocalization between each. Single-plane confocal images from the middle of cells that best reveal stress granules did not always also capture optimal representation of inclusion bodies and viral RNA in that cell (for example, at 12 h p.i.). Therefore, we also provided merge images for these structures at the surface of the same cells (Fig. 7, sixth column).

DISCUSSION

These experiments show that inoculation of human cells with RSV induces stress granules within 12 h of inoculation, and the frequency of stress granules increases with the time since inoculation. Although stress granule formation typically is associated with translation inhibition, resulting in a potentially antiviral state, the findings here show that impairment of stress granule formation by G3BP knockdown reduces RSV replication. In addition, the presence of stress granules was associated with more robust viral protein expression on a per-cell basis. Our data also suggest that even though RSV induces stress granules and these structures contain many RNA binding proteins, the site of viral RNA production is in viral inclusion bodies and not stress granules.

Following attachment and entry, RSV begins its life cycle with gene transcription using an RNA-dependent viral RNA

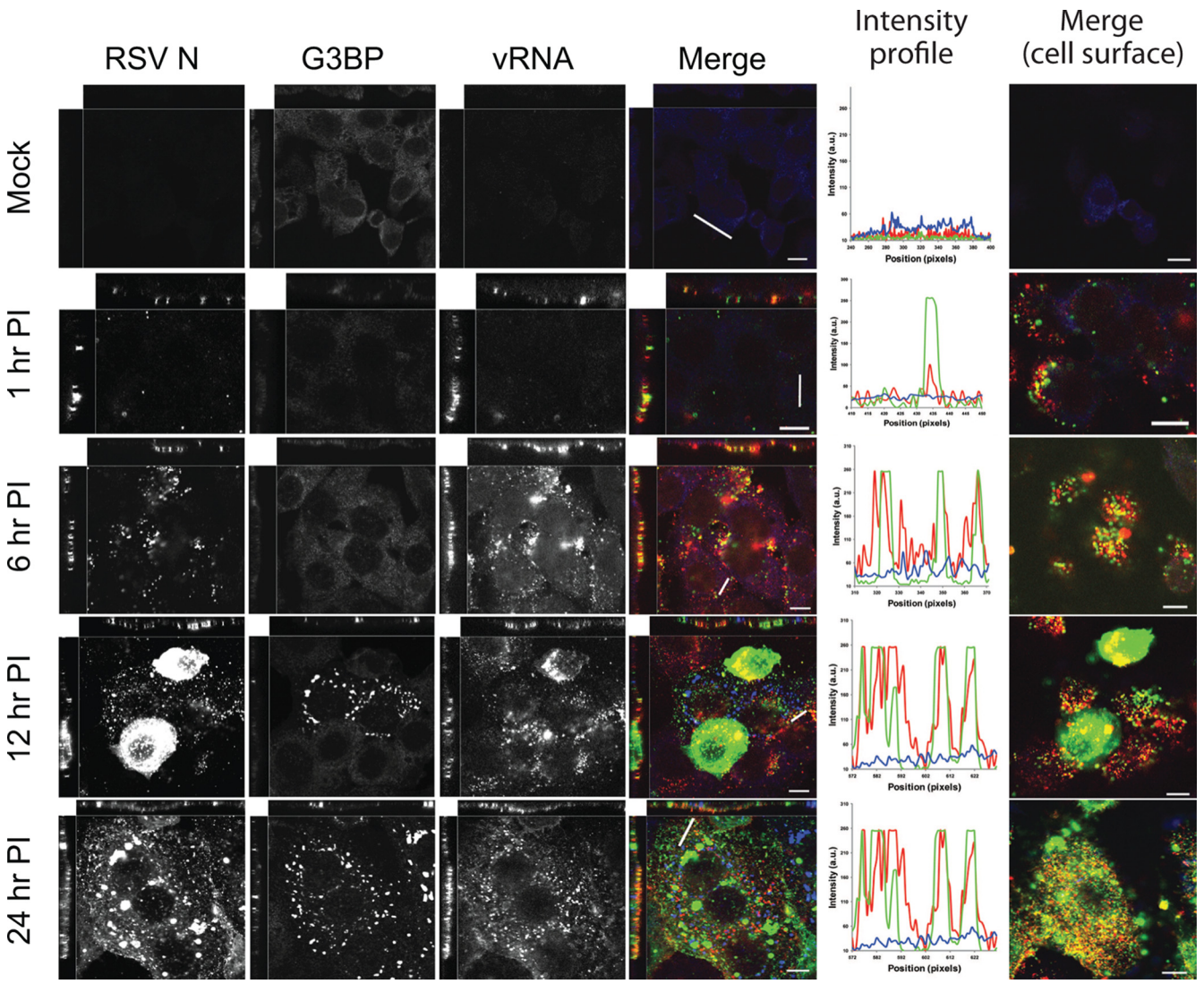

FIG. 7. Viral genomic RNA predominantly colocalizes with RSV inclusion bodies. HEp-2 cells were mock-infected or infected with RSV (MOI = 1) for the indicated times. RSV RNA-specific probes were added as described in Materials and Methods. Cells were fixed and processed for immunofluorescence. Anti-RSV N was used as an inclusion body marker and appears green in the merged image. Anti-G3BP was used as a stress granule marker and appears blue in the merged image. RSV RNA (vRNA) appears red in the merged image (fourth column). The main images are *xy* cross sections, and the images above and to the left represent *xz* and *yz* cross sections, respectively. The horizontal lines are scale bars, while the diagonal or vertical lines were used to calculate the intensity profiles. Intensity profiles at each time point demonstrate the strong correlation between the N protein and viral genomic RNA (fifth column). Images of N (green), viral genomic RNA (red), and G3BP (blue) in mock infection and at 1, 6, 12, and 24 h postinfection at an image plane near the cell surface are in the sixth column. PI, postinfection; a.u., absorbance units.

polymerase. Following the accumulation of viral mRNAs and proteins, the viral polymerase switches from a predominant mode of transcription of mRNAs to replication of the viral genome. Interestingly, our results indicate that stress granule formation begins approximately when RSV initiates this switch.

TABLE 1. RSV RNA is predominantly associated with viral inclusion bodies

Pair of structures analyzed	% Colocalization at time (h) postinfection		
	1	12	24
Viral RNA + inclusion bodies	87	96	91
Viral RNA + stress granules	0.0	2.2	4.5
Inclusion bodies + stress granules	0.0	1.6	3.4

G3BP was first described as an essential stress granule assembly protein through experiments that demonstrated that the overexpression of G3BP results in the spontaneous formation of stress granules (37). In more recent studies, cells in which G3BP expression was modestly reduced, by 30%, using transient small interfering RNA, transfected cells were treated with arsenite. In these experiments, large stress granules without G3BP could be observed in some cells, while other cells contained smaller and fewer stress granules (39). TIA-1 also has been proposed to be an essential stress granule assembly protein. Previous reports demonstrated that TIA-1 knockout mouse embryo fibroblasts treated with arsenite displayed a

diminished capacity to form stress granules (11). It has been proposed that these two proteins mediate stress granule formation in similar ways, because both proteins bind mRNA and both exhibit autoaggregation properties. Other stress granule proteins, such as TIAR (11) and HuR (our studies), have been knocked down but appear to have little effect on stress granule formation. It should be noted that G3BP plays a role in other cellular functions besides stress granule formation. G3BP has been well characterized as a binding partner for Ras GTPase-activating protein (RasGAP), a factor important in cellular proliferation pathways (29). In addition, G3BP is known to be an mRNA binding protein with an endoribonuclease function (8, 38). Thus, knockdown of G3BP may have other unknown consequences for viral replication independent of stress granule formation.

In addition to RSV, parainfluenza virus 5 and Sendai virus are two other paramyxoviruses that are known to induce stress granules (2, 12). In each case, stress granules were shown to be present at relatively late time points after infection (18 to 24 h). This finding is in contrast to results with other viruses, such as poliovirus and Semliki Forest virus, that induce stress granules early after infection but restrict stress granule assembly at later time points (24, 39). Thus, it is possible that stress granule formation enhances paramyxovirus replication during a portion of the viral life cycle. Further evidence of this enhancement comes from our results with G3BP-deficient cells. In these cells, stress granule formation was impaired and, consequently, viral replication was reduced. Other viruses, such as West Nile virus and vaccinia virus, recruit specific proteins involved in stress granule formation, such as TIA-1 and G3BP, respectively, to viral replication factories (6, 13). Our results show that neither TIA-1 nor G3BP associated with RSV RNA and neither protein was recruited to RSV inclusion bodies, which are the likely sites of viral replication.

HuR is a known mRNA binding protein thought to act as a translation enhancer. The protein typically binds AU-rich regions of the 3′ untranslated regions (UTR) of mRNAs and is a known component of stress granules (16). In addition, HuR has been shown to interact with elements of multiple viruses. HuR was shown to bind to the 3′ UTR of HCV (35). Knockdown of HuR resulted in a reduction of HCV replicon RNA (20), indicating a potential role in HCV replication. Recently, HuR was shown to interact with the HIV reverse transcriptase protein (31). When HuR was knocked down, HIV reverse transcription was impaired. Conversely, overexpression of HuR increased HIV reverse transcription. In our studies, although we observed HuR localization in viral inclusion bodies, knockdown of HuR by up to 70% did not affect viral replication. It is thus likely that HuR is not essential for RSV replication, or it is possible that modest levels of this protein can maintain such a role.

Interactions between viral RNA and stress granule proteins have been described. Previous studies have shown that Sendai virus RNA contains TIAR-binding sites, suggesting viral RNA interaction with stress granule proteins (12). The West Nile virus 3′-terminal stem-loop RNA binds TIA-1 and TIAR (22). In addition, we recently showed that RSV RNA interacts transiently with stress granules when infected cells are treated with arsenite (33). In these studies, individual granules of RSV RNA were observed to move into juxtaposition with stress granules, dock, and then separate again. We observed similar transient interactions between RSV RNA and stress granules here; however, our data suggest that viral genomic RNA is much more abundant in viral inclusion bodies.

A detailed understanding of the molecular mechanisms underlying stress granule effects during viral infection is lacking. In fact, evidence exists for both proviral and antiviral roles. When TIA-1 knockout cells that exhibit impaired stress granule formation were infected with vesicular stomatitis virus or Sindbis virus, both viruses grew to higher titers, indicating that TIA-1 or, possibly, stress granules are restrictive to these viruses (22). However, infection of TIAR knockout cells with West Nile virus resulted in decreased viral titers, suggesting a proviral role for this protein. It is important to note, however, that the functional role of stress granules in any sort of stress condition is still not completely understood. Stress granules have been proposed to be sites of mRNA sorting during periods of translation inhibition generated by a variety of stresses (15). While multiple species of mRNA have been shown to be associated with stress granules, this association appears to be transient in nature (17, 19, 23). More recent studies have suggested that mRNA cycles between the cytoplasm and stress granules and that the vast majority of cellular mRNA remains cytoplasmic, suggesting that these structures are neither a holding nor a modification site for mRNAs (26).

Our studies suggest a functional role for stress granules during RSV infection that enhances replication. Further experiments will need to be carried out to determine the exact mechanism of induction and the true role of these structures. The identification of a specific function of stress granules during viral infection could also elucidate a general function for these structures in the normal cell life cycle.

ACKNOWLEDGMENTS

Confocal microscopy imaging experiments were performed in the Vanderbilt Cell Imaging Shared Resources. We thank Paul Anderson for supplying U2OS and RGD3 cells.

This work was supported by a Burroughs Wellcome Fund Clinical Scientist Award in Translation Research (J.E.C.) and the March of Dimes.

REFERENCES

1. **Brown, G., H. W. Rixon, J. Steel, T. P. McDonald, A. R. Pitt, S. Graham, and R. J. Sugrue.** 2005. Evidence for an association between heat shock protein 70 and the respiratory syncytial virus polymerase complex within lipid-raft membranes during virus infection. Virology **338:**69–80.
2. **Carlos, T. S., D. F. Young, M. Schneider, J. P. Simas, and R. E. Randall.** 2009. Parainfluenza virus 5 genomes are located in viral cytoplasmic bodies whilst the virus dismantles the interferon-induced antiviral state of cells. J. Gen. Virol. **90:**2147–2156.
3. **Carromeu, C., F. M. Simabuco, R. E. Tamura, L. E. Farinha Arcieri, and A. M. Ventura.** 2007. Intracellular localization of human respiratory syncytial virus L protein. Arch. Virol. **152:**2259–2263.
4. **Cristea, I. M., J. W. Carroll, M. P. Rout, C. M. Rice, B. T. Chait, and M. R. MacDonald.** 2006. Tracking and elucidating alphavirus-host protein interactions. J. Biol. Chem. **281:**30269–30278.
5. **Dang, Y., N. Kedersha, W. K. Low, D. Romo, M. Gorospe, R. Kaufman, P. Anderson, and J. O. Liu.** 2006. Eukaryotic initiation factor 2alpha-independent pathway of stress granule induction by the natural product pateamine A. J. Biol. Chem. **281:**32870–32878.
6. **Emara, M. M., and M. A. Brinton.** 2007. Interaction of TIA-1/TIAR with West Nile and dengue virus products in infected cells interferes with stress granule formation and processing body assembly. Proc. Natl. Acad. Sci. U. S. A. **104:**9041–9046.
7. **Fields, B. N., D. M. Knipe, and P. M. Howley.** 2007. Fields virology, 5th ed. Lippincott Williams & Wilkins, Philadelphia, PA.
8. **Gallouzi, I. E., F. Parker, K. Chebli, F. Maurier, E. Labourier, I. Barlat, J. P. Capony, B. Tocque, and J. Tazi.** 1998. A novel phosphorylation-dependent

RNase activity of GAP-SH3 binding protein: a potential link between signal transduction and RNA stability. Mol. Cell. Biol. **18:**3956–3965.
9. **Garcia, J., B. Garcia-Barreno, A. Vivo, and J. A. Melero.** 1993. Cytoplasmic inclusions of respiratory syncytial virus-infected cells: formation of inclusion bodies in transfected cells that coexpress the nucleoprotein, the phosphoprotein, and the 22K protein. Virology **195:**243–247.
10. **Garcia-Barreno, B., T. Delgado, and J. A. Melero.** 1996. Identification of protein regions involved in the interaction of human respiratory syncytial virus phosphoprotein and nucleoprotein: significance for nucleocapsid assembly and formation of cytoplasmic inclusions. J. Virol. **70:**801–808.
11. **Gilks, N., N. Kedersha, M. Ayodele, L. Shen, G. Stoecklin, L. M. Dember, and P. Anderson.** 2004. Stress granule assembly is mediated by prion-like aggregation of TIA-1. Mol. Biol. Cell **15:**5383–5398.
12. **Iseni, F., D. Garcin, M. Nishio, N. Kedersha, P. Anderson, and D. Kolakofsky.** 2002. Sendai virus trailer RNA binds TIAR, a cellular protein involved in virus-induced apoptosis. EMBO J. **21:**5141–5150.
13. **Katsafanas, G. C., and B. Moss.** 2007. Colocalization of transcription and translation within cytoplasmic poxvirus factories coordinates viral expression and subjugates host functions. Cell Host Microbe **2:**221–228.
14. **Kedersha, N., and P. Anderson.** 2007. Mammalian stress granules and processing bodies. Methods Enzymol. **431:**61–81.
15. **Kedersha, N., and P. Anderson.** 2002. Stress granules: sites of mRNA triage that regulate mRNA stability and translatability. Biochem. Soc. Trans. **30:**963–969.
16. **Kedersha, N., S. Chen, N. Gilks, W. Li, I. J. Miller, J. Stahl, and P. Anderson.** 2002. Evidence that ternary complex (eIF2-GTP-tRNA(iMet))-deficient preinitiation complexes are core constituents of mammalian stress granules. Mol. Biol. Cell **13:**195–210.
17. **Kedersha, N., G. Stoecklin, M. Ayodele, P. Yacono, J. Lykke-Andersen, M. J. Fritzler, D. Scheuner, R. J. Kaufman, D. E. Golan, and P. Anderson.** 2005. Stress granules and processing bodies are dynamically linked sites of mRNP remodeling. J. Cell Biol. **169:**871–884.
18. **Kedersha, N., S. Tisdale, T. Hickman, and P. Anderson.** 2008. Real-time and quantitative imaging of mammalian stress granules and processing bodies. Methods Enzymol. **448:**521–552.
19. **Kedersha, N. L., M. Gupta, W. Li, I. Miller, and P. Anderson.** 1999. RNA-binding proteins TIA-1 and TIAR link the phosphorylation of eIF-2 alpha to the assembly of mammalian stress granules. J. Cell Biol. **147:**1431–1442.
20. **Korf, M., D. Jarczak, C. Beger, M. P. Manns, and M. Kruger.** 2005. Inhibition of hepatitis C virus translation and subgenomic replication by siRNAs directed against highly conserved HCV sequence and cellular HCV cofactors. J. Hepatol. **43:**225–234.
21. **Li, D., D. A. Jans, P. G. Bardin, J. Meanger, J. Mills, and R. Ghildyal.** 2008. Association of respiratory syncytial virus M protein with viral nucleocapsids is mediated by the M2-1 protein. J. Virol. **82:**8863–8870.
22. **Li, W., Y. Li, N. Kedersha, P. Anderson, M. Emara, K. M. Swiderek, G. T. Moreno, and M. A. Brinton.** 2002. Cell proteins TIA-1 and TIAR interact with the 3′ stem-loop of the West Nile virus complementary minus-strand RNA and facilitate virus replication. J. Virol. **76:**11989–12000.
23. **Mazroui, R., S. Di Marco, R. J. Kaufman, and I. E. Gallouzi.** 2007. Inhibition of the ubiquitin-proteasome system induces stress granule formation. Mol. Biol. Cell **18:**2603–2618.
24. **McInerney, G. M., N. L. Kedersha, R. J. Kaufman, P. Anderson, and P. Liljestrom.** 2005. Importance of eIF2alpha phosphorylation and stress granule assembly in alphavirus translation regulation. Mol. Biol. Cell **16:**3753–3763.
25. **Mokas, S., J. R. Mills, C. Garreau, M. J. Fournier, F. Robert, P. Arya, R. J. Kaufman, J. Pelletier, and R. Mazroui.** 2009. Uncoupling stress granule assembly and translation initiation inhibition. Mol. Biol. Cell **20:**2673–2683.
26. **Mollet, S., N. Cougot, A. Wilczynska, F. Dautry, M. Kress, E. Bertrand, and D. Weil.** 2008. Translationally repressed mRNA transiently cycles through stress granules during stress. Mol. Biol. Cell **19:**4469–4479.
27. **Montero, H., M. Rojas, C. F. Arias, and S. Lopez.** 2008. Rotavirus infection induces the phosphorylation of eIF2alpha but prevents the formation of stress granules. J. Virol. **82:**1496–1504.
28. **Norrby, E., H. Marusyk, and C. Orvell.** 1970. Morphogenesis of respiratory syncytial virus in a green monkey kidney cell line (Vero). J. Virol. **6:**237–242.
29. **Parker, F., F. Maurier, I. Delumeau, M. Duchesne, D. Faucher, L. Debussche, A. Dugue, F. Schweighoffer, and B. Tocque.** 1996. A Ras-GTPase-activating protein SH3-domain-binding protein. Mol. Cell. Biol. **16:**2561–2569.
30. **Raaben, M., M. J. Groot Koerkamp, P. J. Rottier, and C. A. de Haan.** 2007. Mouse hepatitis coronavirus replication induces host translational shutoff and mRNA decay, with concomitant formation of stress granules and processing bodies. Cell Microbiol. **9:**2218–2229.
31. **Rivas-Aravena, A., P. Ramdohr, M. Vallejos, F. Valiente-Echeverria, V. Dormoy-Raclet, F. Rodriguez, K. Pino, C. Holzmann, J. P. Huidobro-Toro, I. E. Gallouzi, and M. Lopez-Lastra.** 2009. The Elav-like protein HuR exerts translational control of viral internal ribosome entry sites. Virology **392:**178–185.
32. **Santangelo, P., N. Nitin, L. LaConte, A. Woolums, and G. Bao.** 2006. Live-cell characterization and analysis of a clinical isolate of bovine respiratory syncytial virus, using molecular beacons. J. Virol. **80:**682–688.
33. **Santangelo, P. J., A. W. Lifland, P. Curt, Y. Sasaki, G. J. Bassell, M. E. Lindquist, and J. E. Crowe, Jr.** 2009. Single molecule-sensitive probes for imaging RNA in live cells. Nat. Methods **6:**347–349.
34. **Smith, J. A., S. C. Schmechel, A. Raghavan, M. Abelson, C. Reilly, M. G. Katze, R. J. Kaufman, P. R. Bohjanen, and L. A. Schiff.** 2006. Reovirus induces and benefits from an integrated cellular stress response. J. Virol. **80:**2019–2033.
35. **Spangberg, K., L. Wiklund, and S. Schwartz.** 2000. HuR, a protein implicated in oncogene and growth factor mRNA decay, binds to the 3′ ends of hepatitis C virus RNA of both polarities. Virology **274:**378–390.
36. **Spann, K. M., K. C. Tran, B. Chi, R. L. Rabin, and P. L. Collins.** 2004. Suppression of the induction of alpha, beta, and lambda interferons by the NS1 and NS2 proteins of human respiratory syncytial virus in human epithelial cells and macrophages [corrected]. J. Virol. **78:**4363–4369.
37. **Tourriere, H., K. Chebli, L. Zekri, B. Courselaud, J. M. Blanchard, E. Bertrand, and J. Tazi.** 2003. The RasGAP-associated endoribonuclease G3BP assembles stress granules. J. Cell Biol. **160:**823–831.
38. **Tourriere, H., I. E. Gallouzi, K. Chebli, J. P. Capony, J. Mouaikel, P. van der Geer, and J. Tazi.** 2001. RasGAP-associated endoribonuclease G3Bp: selective RNA degradation and phosphorylation-dependent localization. Mol. Cell. Biol. **21:**7747–7760.
39. **White, J. P., A. M. Cardenas, W. E. Marissen, and R. E. Lloyd.** 2007. Inhibition of cytoplasmic mRNA stress granule formation by a viral proteinase. Cell Host Microbe **2:**295–305.